Title Page (with Author Details)

Application of Hausdorff fractal derivative to the determination of the vertical sediment concentration distribution

HongGuang Sun[a,c,*], Shiqian Nie[b,c] , Aaron I. Packman[d] , Yong Zhang[e] , Dong Chen[f] , Chengpeng Lu[g] , Chunmiao Zheng[h]

[a] State Key Laboratory of Hydrology-Water Resources and Hydraulic Engineering, Hohai University, Nanjing, Jiangsu 210098, China

[b] College of Mathematics and Systems Science, Shandong University of Science and Technology, Qingdao, Shandong 266590, China

[c] College of Mechanics and Materials, Hohai University, Nanjing, Jiangsu 210098, China

[d] Department of Civil and Environmental Engineering, Northwestern University, Evanston, Illinois, United States

[e] Department of Geological Sciences, University of Alabama, Tuscaloosa, AL 35487, United States

[f] Institute of Geographic Sciences and Natural Resources Research Chinese Academy of Sciences, Beijing 100101, China

[g] College of Hydrology and Water Resources, Hohai University, Nanjing, Jiangsu 210098, China

[h] School of Environmental Science and Engineering, Southern University of Science and Technology, Shenzhen, Guangdong 518055, China

[*] Corresponding author. *E-mail addresses*: shg@hhu.edu.cn (H.G. Sun).

Application of Hausdorff fractal derivative to the determination of the vertical sediment concentration distribution

Abstract:

The Rouse formula and its variants have been widely used to calculate the steady-state vertical concentration distribution for suspended sediment in steady sediment-laden flows, where the diffusive flux is assumed to be Fickian. Turbulent flow, however, exhibits fractal properties, leading to non-Fickian diffusive flux for sediment particles. To characterize non-Fickian dynamics of suspended sediment, the current study proposes a Hausdorff fractal derivative based advection-dispersion equation (HADE) model, where the Fickian diffusive flux in the Rouse model is replaced by a fractal derivative re-scaled using a constant diffusivity. The order of the Hausdorff fractal derivative is designed to characterize the influence of the multi-fractal turbulence structure on sediment diffusion. Applications show that the HADE model, with the analytical solution expressed using a stretched exponential function, can accurately describe the observed vertical concentration profiles for suspended sediment with different sizes. This improvement well captures the non-exponential decay of the vertical sediment concentration in turbulent flow. Further analyses of measured sediment concentration profiles reveal that the Hausdorff fractal order decreases with the Rouse parameter, which describes the stronger impact of turbulent flow and a more uniform sediment concentration profile for smaller particles. Model comparisons also show that the HADE model provides better performance in describing the sediment concentration profiles than the improved Rouse formula and the standard fractional derivative advection-dispersion equation (FADE), which either under- or over-estimates vertical displacement of sediment particles, likely due to coherent turbulent structures.

Key words: Anomalous diffusion; Hausdorff fractal derivative; Vertical concentration distribution; Suspended sediment; Metric transform

1. Introduction

Quantification of the vertical distribution of suspended sediment concentration under turbulent flow conditions, which is one of the essential parts of morphological computations, has been a research focus for decades in the hydraulics and environmental science communities (Cheng et al., 2018; Chien & Wan, 1999; Czuba et al., 2015; Nowacki et al., 2015; Park & Latrubesse, 2015). Various theoretical or empirical formulas have been applied to model the steady-state, vertical density/concentration profile of suspended sediment (Boudreau & Hill, 2020; van Rijn, 1984; Rouse, 1937). For example, Umeyaina (1992) investigated the vertical distribution of suspended sediment in uniform open-channel flow using a mixing length hypothesis, which can fit the experimental data for both fine and coarse sediment particles. Wang and Fu (2004) developed a kinetic model to quantify sediment suspension in solid/liquid two-phase flows, as well as the particle velocity distribution function in steady flows (Fu et al., 2005; Wang & Fu, 2004; Wang & Ni, 1991). Mazumder and Ghoshal (2006) proposed a theoretical model based on the Hunt equation to capture the profiles of velocity and sediment. More information on empirical formulas and theoretical results on the vertical distribution of suspended sediment concentration can be found in related references (Boudreau & Hill, 2020; Dey et al., 2018). The existing formulas are mainly built upon the Fick's law based diffusive flux to describe the vertical movement of suspended sediment (Chien & Wan, 1999; Coleman, 1986; Kumbhakar et al., 2017).

The standard models for the vertical distribution of suspended sediment concentration in sediment-laden flows were derived from the advection-dispersion equation (ADE), which reduces to the following form under steady-state conditions:

$$\omega S + \varepsilon_{sy} \frac{\partial S}{\partial y} = 0, \tag{1}$$

where $S\left[ML^{-1}\right]$ denotes the sediment volumetric concentration, $y\left[L\right]$ is the vertical coordinate, $\omega\left[LT^{-1}\right]$ is the sediment settling velocity, and $\varepsilon_{sy}\left[L^2T^{-1}\right]$ is the sediment turbulent diffusion coefficient along the y direction. Equation (1) assumes that, when reaching equilibrium, the downward settling flux of sediment due to gravity is balanced by upward, Fickian diffusive flux due to turbulence. The diffusion coefficient of sediment, ε_{sy}, whose value cannot be directly measured, was simplified as a parabolic function (Rouse, 1937), a linear function or constant (Larras, 1969), or a parabolic function or constant (van Rijn, 1984). Assuming a parabolic function $\varepsilon_{sy} = \beta\kappa u_* \left(1 - y/h\right) y$ (where u_* is the shear velocity, h is the water depth, and κ is the Von Karman constant), in the solution for the classical Rouse Eq. (1) takes the following form (Rouse, 1937; Vanoni & Brooks, 1957):

$$\frac{S}{S_a} = \left[\frac{\frac{h}{y} - 1}{\frac{h}{a} - 1} \right]^{\frac{\omega}{\beta \kappa u_*}}, \tag{2}$$

where S_a is the reference concentration at reference level a, $\beta = \varepsilon_{sy} / \varepsilon_m$ is the inverse of the sediment Schmidt number, and ε_m is the fluid eddy viscosity. The determination of β is an important topic in the investigation of the vertical distribution of the suspended sediment concentration. Previous literature has revealed that β depends on the normalized settling velocity (Jain et al., 2018), may also depend on the reference level and reference concentration (Pal & Ghoshal, 2016). It may be larger than 1 or less than 1 in different cases (Cellino & Graf, 2002). In current study, $\beta = 1$ is applied when using Eq. (1) for simplicity. Although the Rouse Eq. (1) has a clear physical meaning and has been widely used to study sediment transport, many studies showed that its solution Eq. (2) cannot accurately capture the sediment distribution near the river bottom and surface (Chien & Wan, 1999; Otsuka et al., 2017).

The obvious shortcoming of the Rouse formula motivated various improvements in the last two decades. For example, Wang and Ni (1991) proposed a particle velocity distribution function in two-phase flows, and then derived a theoretical model for the vertical distribution of suspended sediment concentration using the kinetic theory. Cao et al. (1995) analyzed the velocity and sediment concentration distribution in open channel flows using the fundamental two-phase flow equation. Zheng et al. (2012) proposed a continuous distribution formula for suspended sediment concentration by modifying the van Rijn formula (van Rijn, 1984). Chen et al. (2013) found that anomalous turbulent diffusion plays an important role in suspended sediment transport, and further presented a fractional derivative advection-dispersion equation (FADE) model to describe the vertical distribution of suspended sediment concentration in steady turbulent flows. The fractional-derivative model can successfully describe the vertical distribution of suspended sediment concentration based on turbulent diffusion in steady flow (Chen et al., 2013; Kundu, 2018; Nie et al., 2017). However, Sun and Chen (2009) argued that anomalous diffusion in turbulence might be better described by the Hausdorff fractal derivative model (which is introduced in detail in the next section) than the FADE model, because the Hausdorff fractal derivative captures different dynamics for material transport. This conclusion, however, has not been checked against any real-world observations of sediment dynamics. Moreover, although the fractional derivative model has been successfully applied to describe anomalous diffusion, its nonlocal nature requires high computational cost in numerical simulations and is not easy-to-implement for hydrologists and engineers. These challenges may be solved by the new model using the Hausdorff fractal derivative, and, hence, it is an interesting topic to develop and check the fractal model to quantify the complex turbulence structure effects on dynamics of suspended sediment in turbulent flow.

The Hausdorff fractal derivative model has been applied to describe complex dynamics observed in natural systems, including anomalous diffusion (Sun et al., 2017; Liang et al., 2019), soil moisture movement (Sun et al., 2013), turbulent flow (Sun & Chen, 2009), hydrodynamics (Balankin & Elizarraraz, 2012), and other fields (Balankin et al., 2013; Cai et al., 2016; Reyes-Marambio et al., 2016). The Hausdorff fractal derivative (representing a fractal time-space metric transform) is introduced from physics to describe anomalous diffusion (or transport) in a fractal structure (Kanno, 1998; Chen, 2006). Since the turbulent flow structure over rough beds is known to have fractal features, the Hausdorff fractal derivative model may provide an improved physically-based description of anomalous turbulent transport, relative to available models. In addition, the stretched exponential function, which forms the fundamental solution of the Hausdorff fractal derivative model, has been widely confirmed to characterize statistical physical quantities (e.g., velocity, acceleration, structure, and energy) of turbulent flow (La Porta et al., 2001; Kellay, 2017; Zhou et al., 2006). These successful applications and statistical properties of turbulence motivated the current study to extend the Hausdorff fractal derivative to characterize the physical dynamics of suspended sediment transport in steady turbulent flows.

This paper is structured as follows. Section 2 introduces the Hausdorff fractal derivative and the derivation of the Hausdorff fractal derivative model with an analytical solution for suspended sediment transport and the equilibrium concentration distribution in the vertical direction. Section 3 checks the applicability of the newly derived model by fitting two sets of experimental observations for sediment with different sizes. Section 4 discusses parameters of the Hausdorff fractal derivative model, and compares the new model with the improved Rouse model and the standard FADE model using more experimental data. Section 5 summarizes the main conclusions and discusses applications for steady-state vertical dynamics of suspended sediment.

2. Hausdorff fractal derivative model

The Rouse model (1) has two main limitations: 1) a debatable assumption of the Fickian type of turbulent flux and empirical assumptions for the eddy diffusivity, and 2) the inability to extend the suspended sediment distribution all the way to the bed (which results because the near-bed flow structure is more complex owing to wakes and other flow structures resulting from bed roughness). Various studies have confirmed that turbulence structure is complex and often exhibits fractal properties, which satisfy the conditions for the application of the Hausdorff fractal derivative (Lanotte et al., 2015; Sreenivasan & Meneveau, 1986). Further, it has been shown that anomalous turbulent diffusion can be well characterized by the Hausdorff fractal derivative model (Chen, 2006; Sun & Chen, 2009). Therefore, here for the first time the Hausdorff fractal derivative is introduced into the Rouse model, leading to a new formula for quantifying the steady-state vertical distribution of the suspended sediment concentration under steady turbulent flow, which will then be compared in detail with previous models.

The Hausdorff fractal space-time fabric is obtained by metric transform of the standard integer-order space-time fabric. The metric transformation is proposed based on two hypotheses: fractal invariance (meaning that physical laws are invariant under the fractal transformation) and fractal equivalence (where the influence of anomalous environmental fluctuations on physical behavior is assumed to be equal to the fractal time-space transform) (Chen, 2006). Under these hypotheses, the Hausdorff fractal derivative can be restated as the normal derivative using the following metric transform:

$$\begin{cases} \hat{t} = t^{\alpha}, \\ \hat{y} = y^{\gamma}, \end{cases} \tag{3}$$

where α and γ $\left(0 < \alpha, \gamma \leq 1\right)$ represent the order of the Hausdorff fractal derivative in time and space, respectively. The Hausdorff fractal derivative indices α and γ describe the Hausdorff dimensions of fractal time and fractal space, respectively. Here $\alpha = d_f \times d_{sc}$ and

$\gamma = d_f$, where d_f is the fractal dimension of space and d_{sc} is the fractal dimension of regions excluding the holes in the fractal structure, based on the theoretical analysis in the (Kanno, 1998). The metric transform Eq. (3) leads to the following definition of the Hausdorff fractal derivative (Chen 2006; Sun et al., 2013):

$$\begin{aligned} \frac{\partial f(t)}{\partial t^{\alpha}} &= \lim_{t_1 \to t} \frac{f(t_1) - f(t)}{t_1^{\alpha} - t^{\alpha}}, \\ \frac{\partial g(y)}{\partial y^{\gamma}} &= \lim_{y_1 \to y} \frac{g(y_1) - g(y)}{y_1^{\gamma} - y^{\gamma}}. \end{aligned} \tag{4}$$

where $f(t)$ is a function of variable t^{α} and $g(y)$ is a function of variable y^{γ}.

To accurately characterize suspended particle motion in the turbulent flow structure with fractal dimension, it proposed to use the corresponding fractal space-time $\left(y^{\gamma}, t^{\alpha}\right)$. The underling hypothesis is that the diffusion of suspended sediment follows Fick's Law in the fractal dimension $\left(H^{\gamma}\right)$. Under the steady-state condition (where the fractal time t^{α} can be deleted from the equation), the following Hausdorff fractal derivative based advection-dispersion equation (HADE) is obtained to model anomalous diffusion of suspended sediment:

$$\omega S + \bar{\varepsilon}_{sy} \frac{\partial S}{\partial y^{\gamma}} = 0, \tag{5}$$

where $\bar{\varepsilon}_{sy}$ represents a depth-averaged diffusivity which can upscale the depth-dependent ε_{sy} in Eq. (1), considering the fact that anomalous diffusion usually happens in the entire model region (which is also called "nonlocal" in space). This effective diffusivity can be calculated by integrating the depth-variable $\bar{\varepsilon}_{sy}$ in the Rouse model from the reference height a (where a = 0.05 h is widely accepted) to the water surface (y = h) (Chen et al., 2013), and $\omega\left[LT^{-1}\right]$ is the sediment settling velocity (Zhang, 1998) which are expressed by

$$\bar{\varepsilon}_{sy} = \frac{\int_{0.05h}^{h} \kappa u_* \left(1 - y/h\right) y \mathrm{d}y}{0.95h} = \frac{209 \kappa u_* h}{1200}, \tag{6}$$

$$\omega = \sqrt{\left(13.95 \frac{\nu}{d}\right)^2 + 1.09 \frac{\gamma_s - \gamma_w}{\gamma_w} g d} - 13.95 \frac{\nu}{d}. \tag{7}$$

where $\nu\left[L^2 T^{-1}\right]$ is the kinematic viscosity ; $g\left[LT^{-2}\right]$ is the gravitational acceleration; $d\left[L\right]$

is the particle diameter; γ_s and γ_w are the specific weights of sediment and water, respectively. Under the condition $S(y=a)=S_a$, the analytical solution of Eq. (5) can be obtained by using the variable substitution $\left(\hat{y}=y^{\gamma}\right)$

$$\frac{S}{S_a}=e^{-\frac{\omega}{\bar{\varepsilon}_{sy}}\left(y^{\gamma}-a^{\gamma}\right)},0<\gamma\leq 1. \tag{8}$$

Note that the Hausdorff fractal derivative order γ is a parameter in the analytical solution Eq. (8) which cannot be directly measured in the field or using existing flume experiments. Hence, the HADE model Eq. (5) contains one more parameter (γ) compared with the classical Rouse model Eq. (1). Notably, when $\gamma=1$, the Eq. (8) reduces to the exponential expression that has previously been proposed for suspended sediment distributions based on empirical observations (Larras, 1969).

Figure 1 shows the distribution of S/S_a is sensitive to the order of the Hausdorff fractal derivative γ. In general, a smaller γ leads to a larger gradient of the vertical distribution of suspended sediment concentration (representing stronger turbulent diffusion), which can facilitate model fitting for river engineers using the observed concentrations of suspended sediment.

Fig. 1. The normalized concentration S/S_a for suspended sediment (calculated using Eq. (8)) with different fractal indices γ. The other parameters (dimensionless in this case) are the same, which are $\kappa=0.4$, $\bar{\varepsilon}_{sy}=0.007$ (L^2/T), $\omega=0.0047$ (L/T), and $u_*=0.05$ (L/T).

3. Model applications and experimental data analysis

To test the applicability of the HADE model Eq. (5) and its solution Eq. (8) in describing the vertical distribution of suspended sediment concentration, we consider two groups of experimental data were considered for natural sands (with different sizes) in fully developed, steady open-channel flows. To evaluate the difference between the experimental data and the model predictions, the root mean square error (RMSE) was used. More experimental data is checked in the next section. The experiments done by Einstein and Chien (1955) and Coleman (1986) are used for comparative purposes. The flow and sediment characteristics of the experiments are listed in Table 1.

Table 1. Flow and sediment characteristics in the experiments of Einstein and Chien (1955) and Coleman (1986).

Run Number	Depth, h (cm)	Particle size, d (mm)	Shear velocity, u_* (cm/s)	Settling velocity, (cm/s)	Von Karman Constant, κ
S-1	13.8	1.300	11.47	13.96	0.322
S-2	12.0	1.300	12.85	13.96	0.261
S-3	11.7	1.300	13.26	13.96	0.246
S-4	11.5	1.300	14.28	13.96	0.210
S-6	14.3	0.94	11.82	11.29	0.295
S-7	14.3	0.94	11.79	11.29	0.281
S-8	13.9	0.94	11.53	11.29	0.263
S-9	13.5	0.94	11.85	11.29	0.247
Coleman 2	17.1	0.105	4.1	0.673	0.403
Coleman 6	17.0	0.105	4.1	0.673	0.410
Coleman 15	17.1	0.105	4.1	0.673	0.414
Coleman 16	17.1	0.105	4.1	0.673	0.432
Coleman 22	17.0	0.210	4.1	2.35	0.457
Coleman 23	17.0	0.210	4.1	2.35	0.453
Coleman 26	17.1	0.210	4.1	2.35	0.466
Coleman 27	16.8	0.210	4.1	2.35	0.446

3.1. Experimental Case 1

This experiment was conducted in two-dimensional, fully developed, steady open-channel flows (Einstein & Chien, 1955). The mean size of sediment particles was 1.3 mm for experimental runs S-1 ~ S-4 and 0.94 mm for S-6 ~ S-9, representing coarse and medium sand, respectively. Detailed information on the experiment can be found in Fu et al. (2005). Here the applicability of the HADE model Eq. (8) is examined and the HADE model is compared with the classical Rouse model Eq. (2). The reference height is selected at a = 0.02 h. The best-fit results of the HADE model (obtained by minimizing the RMSE) for the experimental datasets S-1 ~ S-4 and S-6 ~ S-9 are depicted in Figs. 2 and 3, respectively. Figures 2 and 3 show that the HADE model generally matches the experimental data better than the Rouse model, especially for the regions near the river bed and surface. The improved performance of the HADE model is attributed to its improved ability to capture anomalous diffusion of sediment particles, which is driven by turbulent bursting and cannot be efficiently characterized by the use of Fick's law for diffusive fluxes in the Rouse model.

Fig. 2. Case 1: Comparison of the vertical distribution of suspended sediment concentration fitted by the two models (the HADE model Eq. (8) and the classical Rouse model Eq. (2)) and the experimental data. The mean sediment size is d = 1.3 mm, and the Hausdorff fractal order is $\gamma = 0.93$ for dataset S-1, and $\gamma = 0.99$ for datasets S-2 ~ S-4, with the reference height at a = 0.02 h (experimental data from Einstein and Chien (1955)).

Fig. 3. Case 1: Comparison of the vertical distribution of suspended sediment concentration fitted by the two models (the HADE model Eq. (8) and the classical Rouse model Eq. (2)) and the experimental data. The mean sediment size is d = 0.94 mm, and the Hausdorff fractal order is $\gamma = 0.80$ for datasets S-6 and S-7, and $\gamma = 0.88$ for datasets S-8 and S-9, with the reference height a = 0.02 h (experimental data from Einstein (1955)).

3.2. Experimental Case 2

This experiment was done in a uniform flume, where the mean sediment size is 0.105 mm for Coleman Runs 2, 6, 15, and 16, and 0.210 mm for Coleman Runs 22, 23, 26, and 27, belonging to fine particles and medium particles (Coleman, 1986). Figures 4 and 5 provide the best-fit results of the HADE model for the four runs of each experiment. Similar to Case 1, here the fitting results also show that the HADE model can fit well the experimental data. The best-fit Hausdorff fractal derivative order is $\gamma = 0.73$ for Coleman 2, $\gamma = 0.65$ for Coleman 6, $\gamma = 0.53$ for Coleman 15, $\gamma = 0.51$ for Coleman 16, and $\gamma = 0.99$ for Coleman 22, 23, 26, and 27. This finding implies that fine particles experience stronger super-diffusion than medium sediment particles, because a fine particle has a higher probability to travel a long distance in turbulent flows.

Fig. 4. Case 2: Comparison of the vertical distribution of suspended sediment concentration fitted by the two models (the HADE model Eq. (8) and the classical Rouse model Eq. (2)) and the experimental data, where the sediment diameter is *d* = 0.105 mm, the best-fit fractal order: (a) $\gamma = 0.73$; (b) $\gamma = 0.65$; (c) $\gamma = 0.53$; (d) $\gamma = 0.51$ and the reference height is *a* = 0.02 *h* (experimental data from Coleman (1986)).

Fig. 5. Case 2: Comparison of the vertical distribution of suspended sediment concentration fitted by the two models (the HADE model Eq. (8) and the classical Rouse model Eq. (2)) and the experimental data, where the sediment diameter is *d* = 0.210 mm, the best-fit fractal order is $\gamma = 0.99$, and the reference height is *a* = 0.02 *h* (experimental data from Coleman (1986)).

4. Discussion

4.1. Impact of parameters on sediment profiles and their correlation in the HADE model

In this section, a number of available data sets are used to explore the impact of the Hausdorff fractal derivative order γ and the Rouse parameter ($\omega/\kappa u_*$) on vertical distributions of sediment, as well as the relation between these two major parameters in the HADE model. Four data sets representing a wide range of turbulent flow conditions and sediment sizes (from medium silt to very coarse sand) were selected, including the experimental data derived from Einstein and Chien (1955) (denoted as Case A for description simplicity), Coleman (1986) (denoted as Case B), Wang and Qian (1989, 1992) (denoted as Case C), and the authors measurements at Jianli Station of the Jingjiang River Reach (i.e., the upstream section of the Yongtze River), China (denoted as Case D).

The fractal index γ in the HADE model is the core parameter describing the influence of turbulent bursting on suspended sediment, making estimation of this parameter important for application. The best-fit parameter γ listed in Table 2 varies from 0.51 to 0.99, depending on the turbulence characteristics and the sediment dimension.

The measured Rouse parameter, $\omega/\kappa u_*$, listed in Table 2, which is a ratio characterizing the gravity and turbulent diffusion effects, ranges from 0.3800 to 4.6558. It affects the shape of the vertical profile for suspended sediment. An increase in the Rouse parameter, representing decreased dispersion relative to particle advection, results in a profile of suspended sediment with higher nonuniformity.

Table 2. Values for the best-fit Hausdorff fractal derivative index γ in the HADE model, the measured sediment diameter, *d*, and the measured Rouse parameter ($\omega/\kappa u_*$). The detailed fitting results of the HADE model using the experimental and field measurement data are provided in Appendix A.

Run number	Hausdorff fractal derivative index γ	Particle size *d* (mm)	Rouse parameter $\omega/\kappa u_*$
A1	0.93	1.300	3.7803
A2	0.99	1.300	4.1629
A3	0.99	1.300	4.2802
A4	0.99	1.300	4.6558
A5	0.80	0.940	3.2375
A6	0.80	0.940	3.4074
A7	0.88	0.940	3.7227
A8	0.88	0.940	3.8568
A9	0.82	0.274	0.9425
A10	0.85	0.274	1.3547
A11	0.86	0.274	1.4652
A12	0.86	0.274	1.2295
A13	0.88	0.274	1.4484
B1	0.73	0.105	0.4073
B2	0.65	0.105	0.4004
B3	0.53	0.105	0.3965
B4	0.51	0.105	0.3800
B5	0.99	0.210	1.2542
B6	0.99	0.210	1.2563
B7	0.99	0.210	1.2300
B8	0.99	0.210	1.2851
C1	0.98	0.150	0.6411
C2	0.97	0.150	0.6377
C3	0.96	0.150	0.6576
C4	0.99	0.960	0.5427
D1	0.98	0.375	1.2885
D2	0.80	0.175	1.6268
D3	0.78	0.075	1.1969
D4	0.56	0.025	0.7353

The foregoing experimental data, grouped based on the sediment size (see Table 2), show that the Hausdorff fractal order, γ , increases approximately linearly with the Rouse parameter ($\omega/\kappa u_*$)

(Fig. 6). This positive relation might be due to the fact that a smaller γ or a smaller $\omega/\kappa u_*$ can generate a more uniform vertical distribution of suspended sediment, which represents strong super-diffusion (upward jumps) due to turbulent coherent structures. But a universal regression model cannot be proposed based on the existing experimental data and limited knowledge. On one hand, as shown by Fig. 1, the fractal order γ controls the overall trend of the sediment vertical profiles. When $\gamma \to 1$ (i.e., weak turbulence), the suspended sediment distributes as an exponential function with more mass near the river-bed. A smaller γ indicates more anomalous transport of suspended sediment caused by stronger upward jumps that rapidly move the bottom sediment upward. When $\gamma \to 0$ (i.e., strong turbulence), sediment distributes uniformly along the vertical direction with a constant concentration $S/S_a = 1$. On the other hand, the Rouse parameter, $\omega/\kappa u_*$, acts as a scaling factor that controls the expansion of the sediment vertical profile: a smaller $\omega/\kappa u_*$ indicates more anomalous transport of suspended sediment caused by stronger diffusive jumps (compared to advective jumps), which can smooth the sediment profile by decreasing the vertical concentration gradient. The sensitivity of the sediment vertical profile to $K = \omega/\bar{\varepsilon}_{sy}$ is shown in Fig. 7. Figure 7 shows that a smaller $\omega/\bar{\varepsilon}_{sy}$, likely resulting from stronger turbulence, enhances anomalous transport (i.e., fast displacement) and results in a more uniform vertical concentration distribution.

Fig. 6. The relation between the Hausdorff fractal derivative index γ (fitted) and the Rouse parameter $\omega/\kappa u_*$ (measured). The line represents the best-fit linear relation for the various datasets (symbols).

Fig. 7. Effect of $K = \omega/\bar{\varepsilon}_{sy}$ on the vertical distribution of suspended sediment (for Run S-8, *d* = 0.94 mm, $\gamma = 0.88$, and $K = \omega/\bar{\varepsilon}_{sy} = 153.7739$, of the experimental data from Einstein and Chien (1955)).

It can be seen that both the fractal order, γ, and the Rouse parameter, $\omega/\kappa u_*$, define the smoothness of sediment distribution. Notably, Fig. 6 implies that the suspension index, $\omega/\kappa u_*$, is not the only factor that can affect the Hausdorff fractal order. Other factors including the mean flow velocity and Reynolds number also play an important role in the random motion of suspended particles in turbulent flows, generating, therefore, the sediment profile and determining the value of γ.

4.2. Model comparison

The sediment Schmidt number, β, in the Rouse model relates the sediment diffusivity to the fluid eddy viscosity under steady-state and uniform flow conditions. Adjusting β in the classical Rouse model may reconcile the model solution to the measured data (Nie et al., 2017). In open channel flows, β may characterize the complex interactions between the fluid and the solid sediment grains in suspension. It may also act as a correction factor to fix the intrinsic modeling error due to the inability to directly simulate all relevant fluid-particle interactions based on real-world physical information (e.g., turbulence damping, hindered settling, and mobile-bed effects). Hence, an improved model for the Rouse formula can be obtained by adjusting β.

Here the following formula is used to calculate β (Cheng et al., 2013)

$$\beta = \frac{1+\lambda Z}{1+\xi/Z} \tag{9}$$

where $Z = \frac{\omega}{\kappa u_*}$ is the Rouse parameter, the factor $\lambda = 1$, and $\xi = 0.034$. Pal and Ghoshal (2016) developed a new expression for β, which is denoted as:

$$\beta = 2.204\left(\frac{\omega}{u_*}\right)^{0.667} a^{0.178} S_a^{\ 0.017}. \tag{10}$$

For comparison, the improved Rouse model and the M1 model has been obtained by using Eq. (9) and Eq. (10) to modify the Rouse model, respectively.

Fig. 8. Solutions of three models (HADE, Improved Rouse, and M1 models) compared with the experimental data. The mean particle size is *d* = 0.94 mm, the Hausdorff fractal order is $\gamma = 0.93$, $\beta = 1.3657$ in the improved Rouse model, $\beta = 1.4371$ in the M1 model, and *a* = 0.02 *h* (experimental data from Einstein and Chien (1955)).

The results show that the improved Rouse model can only adjust part of the sediment profile, especially the intermediate section, while the overall trend of the profile cannot be adjusted significantly (Appendix A). One example is shown in Fig. 8, where the improved Rouse model and M1 model still cannot capture the overall sediment concentration profile, and the HADE model provides a better fit to the measured data than the improved Rouse model.

The FADE model has been used to describe the vertical distribution of suspended sediment in steady turbulent flow (Chen et al., 2013) as follows:

$$\omega S + \bar{\varepsilon}_{sy} \frac{\partial^{\eta} S}{\partial y^{\eta}} = 0, \tag{11}$$

where η $\left(0 < \eta \leq 1\right)$ (dimensionless) denotes the order of the Caputo-type fractional derivative. The analytical solution of Eq. (11) is as follows (Chen et al., 2013):

$$\frac{S}{S_a} = E_{\eta}\left(-\frac{\omega}{\bar{\varepsilon}_{sy}}\left(y-a\right)^{\eta}\right), \tag{12}$$

Atangana and Baleanu (2016) developed the fractional derivative with Mittag-Leffler function kernel, which is defined as follows (Yu et al., 2018):

$${}^{ABC}_{\ a}D^{\eta}_{y} f\left(y\right) = \frac{B\left(\eta\right)}{1-\eta}\int_{a}^{y} f'\left(\tau\right) E_{\eta}\left[-\eta\frac{\left(y-\tau\right)^{\eta}}{1-\eta}\right] d\tau. \tag{13}$$

where $B\left(\eta\right)$ is a normalization function, ${}^{ABC}_{\ a}D^{\eta}_{y}$ is the Caputo fractional derivative which defined by the Atangana and Baleanu (2016). $f'\left(y\right)$ is the first derivative of function $f\left(y\right)$, τ is the integral variable. So the corresponding Rouse equation can be expressed as:

$$\omega S + \bar{\varepsilon}_{sy}\ {}^{ABC}_{\ a}D^{\eta}_{y} S = 0 \tag{14}$$

Then the analytical solution of Eq. (14) can be expressed as:

$$\frac{S}{S_a} = \frac{1}{1+\frac{\omega}{\bar{\varepsilon}_{sy}}-\frac{\omega}{\bar{\varepsilon}_{sy}}\eta} E_{\eta}\left[\frac{-\frac{\omega}{\bar{\varepsilon}_{sy}}\eta}{1+\frac{\omega}{\bar{\varepsilon}_{sy}}-\frac{\omega}{\bar{\varepsilon}_{sy}}\eta}\left(y-a\right)^{\eta}\right]. \tag{15}$$

where $E_{\eta}\left(z\right)$ denotes the Mittag-Leffler function, which can be written as:

$$E_{\eta}\left(z\right) = \sum_{k=0}^{\infty}\frac{z^{k}}{\Gamma\left(\eta k+1\right)} \tag{16}$$

The comparison results of three models is shown in Fig. 9.

Fig. 9. Solutions of three models (HADE, Fractional, and ABC Fractional models) compared with the experimental data. The mean particle size is d = 1.3 mm, $\gamma = 0.93$ in the HADE model, $\eta = 0.91$ in the Fractional model, $\eta = 0.9996$ in the ABC Fractional model, and a = 0.02 h (experimental data from Einstein (1955)).

The FADE model Eq. (11) differs from the HADE model Eq. (5) in at least two ways. First, the FADE model considers the nonlocality of particle motion in turbulence, while the HADE model is built upon a metric transform between normal and fractal structures. Second, the FADE model leads to a Mittag-Leffler (or power-law) type of sediment distribution, while the HADE model produces a stretched exponential distribution. The power-law density function for random motion yields much larger jumps, whereas the stretched exponential density function is weighted more towards smaller motions and is not heavy-tailed. This discrepancy results in the calculated concentration of the HADE model declining relatively faster than the standard FADE model. Suspended particles may move upward with coherent flow structures such as Kolk-Boil vortices while undergoing settling, resulting in a travel path distribution "lighter" than the power-law distribution assumed typically for cascade eddies, which suggests that the HADE model better describes the underlying motion than the standard FADE model. It is also worthwhile to emphasize that the stretched exponential density function is more physically justified here, since turbulence structures have defined scales (i.e., they break up or dissipate to the background turbulence). It is expected that this limited extent of non-locality can be better represented by a stretched-exponential model (i.e., the HADE model).

Comparison among the HADE model, the FADE model (fractional derivative order, η), and the improved Rouse model is shown in Fig. 10. The results show that the HADE model and the FADE model match the data better than the improved Rouse model, and the HADE model gives better fitting results than the FADE model. Generally speaking, the FADE model describes a pure power-law distribution of vertical particle jumps, which overpredicts the vertical transport observed in the sediment profiles. The improved Rouse model with a adjustable Schmidt number can only slightly modify the intermediate range of the sediment profiles. The HADE model describes the particle's vertical travel path distribution in the form of a stretched exponential function, which better matches the measured concentration distributions. Direct measurements of particle vertical jumps under different flow conditions are needed to confirm the best mathematical description for sediment vertical diffusion in turbulent flows, as well as to better predict transport parameters (e.g., the Rouse parameter) for practical field applications in the future.

Fig. 10. Solutions of three models (HADE, Fractional, and ABC Fractional models) compared with the experimental data. (a) d = 1.3 mm, $\gamma = 0.93$ in the HADE model, $\eta = 0.91$ in the FADE model, and $\beta = 1.3657$ in the improved Rouse model; and (b) d = 0.94 mm, $\gamma = 0.88$ in the HADE model, $\eta = 0.88$ in the FADE model, and $\beta = 1.3599$ in the improved Rouse model. The parameter a = 0.02 h (experimental data from Einstein and Chien (1955)).

4.3. Physical interpretation of particle jumps and feasibility of the HADE model

The main assumption applied in the HADE model Eq. (5) is that the jump size distribution (or the travel path distribution during a single jump event) for suspended sediment particles follows a stretched exponential function, which is relatively lighter than the heavy-tailed (i.e., power-law) distribution assumed by the FADE model Eq. (11). Coherent turbulent structures (such as Kolk-Boil vortices, which are the underwater vortices created by rushing water passing an obstacle at the river-bed which can pluck sediment) may initiate from bed roughness elements and propagate upward in the water column, resulting in random vertical transport for suspended sediment particles that is "heavier" than the exponential distribution described by the classical Fickian diffusive flux. The random vertical jump of sediment particles, therefore, might be affected by the competition between gravity (which generates the settling velocity) and the stable vortices. While some of the vortices can reach the free surface of the water and result in a heavy-tailed distribution of travel paths over the entire water column, sediment particles might not completely follow these structures because of the concurrent downward settling. Hence, some of the particles may "drop out" of the vortex before reaching the water surface, resulting in a lighter than heavy-tail or power-law distribution (such as the stretched exponential function) of vertical particle jumps.

Limitations from the system geometry also suggest that a stretched exponential function is more appropriate than a heavy-tailed power law in capturing suspended particle movement in a finite bounded domain. The power-law distributed large displacements (with an infinite variance) of sediment particles would require large-scale, long-term coherent structures throughout the water column, but these structures are limited by the vertical boundaries, resulting in a new distribution with a finite variance such as the stretched exponential function. Such a truncation is common in hydrological processes, such as the truncated jumps for particles moving in fluvial systems where the ancient channel and floodplain deposits have a finite size (Zhang, 2010; Zhang & Meerschaert, 2011).

In summary, the HADE model may better capture suspended sediment dynamics than either the standard FADE model (which assumes pure power-law jumps for particles driven by eddy cascades) or the Rouse model (which assumes that Fickian diffusion governs upward particle motion). These hypotheses need further validation, especially additional observations or simulation of the vertical jump distributions for suspended particle transport in rivers.

It is also noteworthy that none of the suspended sediment transport studies that were analyzed in the current study provided observed turbulence structures or turbulence velocity fluctuations, and, hence, here only the qualitative relationship between the Hausdorff index, γ, and turbulence properties can be proposed. Scale analysis of the Hausdorff model and its index γ based on turbulence intensity and energy and space-time scales of coherent structures remains an open research question.

5. Conclusions

Suspended sediment exerts an important control on geomorphological and biogeochemical processes in rivers. Efficient quantification of suspended sediment dynamics remains a challenge. A non-Fickian transport model is proposed as an alternative to the classical Rouse model to capture complex dynamics for suspended sediment in steady sediment-laden flows. Model development, numerical analysis, real-world validation, and model comparison reveal the following three main conclusions.

First, a HADE model, which is built upon the Hausdorff fractal derivative and can be solved analytically, is proposed to capture the steady-state vertical distribution of suspended sediment.

This novel stochastic model contains a single fitting parameter, the fractal order γ, to efficiently characterize non-Fickian dynamics likely due to turbulent flows. The fractal order can also capture the size-selective behavior of suspended sediment dynamics.

Second, the fractal order controls the overall shape of the suspended sediment concentration profile, and the Rouse parameter (which is a measurable parameter in the HADE model) controls the spatial expansion of this profile. These two parameters are strongly correlated, which may improve the prediction performance of the HADE model. The full predictability of the complex stochastic process for suspended sediment, however, requires much more direct information on the motion of suspended particles in turbulent flows.

Third, model comparisons show that the HADE model can fit the sediment concentration profiles better than both the improved Rouse formula and the standard FADE model, which either under- or over-estimates the vertical displacement of sediment particles in coherent turbulent structures. The competition between gravity and large-scale, long-term vortices, or the finite river depth, can limit large jumps of sediment particles and result in a jump size distribution "lighter" than the power-law function and "heavier" than the exponential function, motivating the application of the stretched exponential function in the HADE model. Further tests and experimental data are needed to check the feasibility of the HADE model for different river flows and morphologies.

Acknowledgments

This research was supported by the National Natural Science Foundation of China (Grants No. 11972148), and the Fundamental Research Funds for the Central Universities (Grants No. B210202092).

Appendix A. Additional model results and comparison

This appendix shows the best-fit results using the HADE model Eq. (5) and the other models for experimental and field measurement data listed in Table 2. Figures A1, A2, and A3 show the model results for the experimental sediment profiles measured by Einstein and Chien (1955), Wang and Qian (1989, 1992), and the authors' field test, respectively. The RMSEs for the HADE model Eq. (5), the FADE model Eq. (11), and the improved Rouse model are listed in Table A1. Both the figures and RMSEs indicate that, for most cases, the HADE model can fit the sediment concentration profiles better than the improved Rouse formula and the FADE model, a conclusion consistent with that found in the main text.

To evaluate the fitting results of the models, the root mean square error (RMSE) is calculated as follow:

$$\mathrm{RSME} = \sqrt{\frac{1}{N}\sum_{i=1}^{N}\left(S_{i0} - S_{ie}\right)^2} \tag{17}$$

where S_{i0} represents the measured sediment concentration, S_{ie} represents the simulated sediment concentration, and N is the number of measured concentration data at the observation point.

Fig. A1. Comparison of the vertical distribution of suspended sediment concentration computed using three models (HADE, Fractional (FADE), and Improved Rouse models), and the experimental data from Einstein and Chien (1955) for d = 0.274 mm. The best-fit parameters are: (a) $\gamma = 0.82$ in the HADE model, $\eta = 0.81$ in the fractional-derivative model, and $\beta = 1.0562$ in the improved Rouse model; (b) $\gamma = 0.85$, $\eta = 0.84$, and $\beta = 1.1077$; (c) $\gamma = 0.86$, $\eta = 0.84$, and $\beta = 1.1205$; (d) $\gamma = 0.86$, $\eta = 0.84$, and $\beta = 1.0927$; and (e) $\gamma = 0.88$, $\eta = 0.86$, and $\beta = 1.1186$.

Fig. A2. Comparison of the vertical distribution of suspended sediment concentration computed using three models (HADE, Fractional (FADE), and Improved Rouse models), and the experimental data from Wang and Qian (1989, 1992) for the sediment sizes d = 0.150 mm for SQ1 ~ SQ3, and d = 0.96 mm for SM1. The best-fit parameters are: (a) $\gamma = 0.98$ in the HADE model, $\eta = 0.96$ in the fractional-derivative model, and $\beta = 1.0105$ in the improved Rouse model; (b) $\gamma = 0.97$, $\eta = 0.95$, and $\beta = 1.0099$; (c) $\gamma = 0.96$, $\eta = 0.95$, and $\beta = 1.0134$; and (d) $\gamma = 0.99$, $\eta = 0.97$, and $\beta = 0.9921$.

Fig. A3. Comparison of the vertical distribution of suspended sediment concentration computed using three models (HADE, Fractional (FADE), and Improved Rouse models), and field data from Jingjiang River at Jianli. (a) The mean sediment size d = 0.375 mm, $\gamma = 0.98$ in the HADE model, $\eta = 0.98$ in the fractional-derivative model, and $\beta = 1.0998$ in the improved Rouse model; (b) d = 0.175 mm, $\gamma = 0.80$, $\eta = 0.90$, and $\beta = 1.1389$; (c) d = 0.075 mm, $\gamma = 0.78$, $\eta = 0.85$, and $\beta = 1.0888$; and (d) d = 0.025 mm, $\gamma = 0.56$, $\eta = 0.63$, and $\beta = 1.0621$.

Table A1. The root mean square errors of fitting results using the HADE model, FADE model and the improved Rouse model for three groups of measurement data (note: S-1 ~ S-15 from Einstein and Chien (1955), SQ1 ~ SQ3 and SM1 from Wang and Qian (1989, 1992), and Jianli1 ~ Jianli4 from the Jianli Station on the Jingjiang River).

Run number	RMSE (HADE model)	RMSE (FADE model)	RMSE (Improved Rouse model)
S-1	0.1072	0.1324	0.4076
S-8	0.2745	0.3034	0.9391
S-11	0.0312	0.0310	0.0613
S-12	0.1605	0.2220	0.5689
S-13	0.4639	0.5167	0.7777
S-14	0.2238	0.6448	1.2038
S-15	0.9531	1.3673	2.3313
SQ1	0.2052	0.1816	0.1932
SQ2	0.5886	0.4736	1.3918
SQ3	0.4390	0.3892	2.1554
SM1	0.0070	0.0075	0.0197
Jilanli1	0.0122	0.0124	0.0030
Jilanli2	0.0268	0.0203	0.0358
Jilanli3	0.0176	0.0142	0.0299
Jilanli4	0.0729	0.0568	0.1931

References

Atangana, A., & Baleanu, D. (2016). New fractional derivatives with nonlocal and non-singular kernel: Theory and application to heat transfer model. *Thermal Science*, *20*, 763–769.

Balankin, A. S., & Elizarraraz, B. E. (2012). Map of fluid flow in fractal porous medium into fractal continuum flow. *Physical Review E*, *85*, 1–21.

Balankin, A. S., Mena, B., Patiño, J., & Morales, D. (2013). Electromagnetic fields in fractal continua. *Physics Letters A*, *377*, 783–788.

Boudreau, B. P., & Hill, P. S. (2020). Rouse revisited: The bottom boundary condition for suspended sediment profiles. *Marine Geology*, *419*, 1–7.

Cai, W., Chen, W., & Xu, W. (2016). Characterizing the creep of viscoelastic materials by fractal derivative models. *International Journal of Non-Linear Mechanics*, *87*, 58–63.

Cao, Z., Wei, L., & Xie, J. (1995). Sediment-laden flow in open channels from two-phase flow viewpoint. *Journal of Hydraulic Engineering*, *121*, 725–735.

Cellino, M., & Graf, W. (2002). Suspension flow in open channels. *Journal of Hydraulic Research*, *15*, 435–447.

Chen, D., Sun, H., & Zhang, Y. (2013). Fractional dispersion equation for sediment suspension. *Journal of Hydrology*, *491*, 13–22.

Chen, W. (2006). Time-space fabric underlying anomalous diffusion. *Chaos, Solitons & Fractals* *28*, 923–929.

Cheng, C., Song, Z., Wang, Y., & Zhang, J. (2013). Parameterized expressions for an improved Rouse equation. *International Journal of Sediment Research*, *28*, 523–534.

Cheng, Z., Chauchat, J., Hsu, T. J., & Calantoni, J. (2018). Eddy interaction model for turbulent suspension in Reynolds-averaged Euler-Lagrange simulations of steady sheet flow. *Advances in Water Resources*, *111*, 435–451.

Chien, N., & Wan, Z. (1999). *Mechanics of sediment transport*. Reston, VA, U.S.: ASCE Press.

Coleman, N. L. (1986). Effects of suspended sediment on the open-channel velocity distribution. *Water Resources Research*, *22*, 1377–1384.

Czuba, J. A., Straub, T. D., Curran, C. A., Landers, M. N., & Domanski, M. M. (2015). Comparison of fluvial suspended-sediment concentrations and particle-size distributions measured with in-stream laser diffraction and in physical samples. *Water Resources Research*, *51*, 320–340.

Dey, S., Ali, S. Z., & Padhi, E. (2018). Advances in analytical modeling of suspended sediment transport. *Journal of Hydro-Environment Research*, *20*, 110–126.

Einstein, H. A; & Chien, N. (1955). Effect of heavy sediment concentration near the bed on velocity and sediment distribution. University of California, Berkeley, CA. Sediment Series No. 8, Omaha, NE. U.S. Army Crops of Engineers, Missouri River Division.

Fu, X., Wang, G., & Shao, X. (2005). Vertical dispersion of fine and coarse sediments in turbulent open-channel flows. *Journal of Hydraulic Engineering*, *131*, 877–888.

Jain, P., Kumbhakar, M., & Ghoshal, K. (2018). A mathematical model on depth-averaged β-factor in open-channel turbulent flow. *Environmental Earth Sciences*, *77*, 1–10.

Kanno, R. (1998). Representation of random walk in fractal space-time. *Physica A: Statistical Mechanics and its Applications*, *248*, 165–175.

Kellay, H. (2017). Hydrodynamics experiments with soap films and soap bubbles: A short review of recent experiments. *Physics of Fluids*, *29*, 1–10.

Kumbhakar, M., Ghoshal, K., & Singh, V. P. (2017). Derivation of Rouse equation for sediment concentration using Shannon entropy. *Physica A: Statistical Mechanics and its Applications*, *465*, 494–499.

Kundu, S. (2018). Suspension concentration distribution in turbulent flows: An analytical study using fractional advection–diffusion equation. *Physica A: Statistical Mechanics and its Applications*, *506*, 135–155.

La Porta, A., Voth, G. A., Crawford, A. M., Alexander, J., & Bodenschatz, E. (2001). Fluid particle accelerations in fully developed turbulence. *Nature*, *409*, 1017–1019.

Lanotte, A. S., Benzi, R., Malapaka, S. K., Toschi, F., & Biferale, L. (2015). Turbulence on a fractal Fourier set. *Physical Review Letters*, *115*, 1–5.

Larras, J. (1969). A new examination of sediment suspension in open channels. *Journal of Hydraulic Research*, *7*, 69–82.

Liang, Y., Wang, S., Chen, W., Zhou, Z., & Magin, R. L. (2019). A survey of models of ultraslow diffusion in heterogeneous materials. *Applied Mechanics Review*s, *71*, 1–16.

Mazumder, B., & Ghoshal, K. (2006). Velocity and concentration profiles in uniform sediment-laden flow. *Applied Mathematical Modelling*, *30*, 164–176.

Nie, S., Sun, H., Zhang, Y., Chen, D., Chen, W., Chen, L., & Schaefer, S. (2017). Vertical distribution of suspended sediment under steady flow: Existing theories and fractional derivative model. *Discrete Dynamics in Nature and Society*, *2017*, 1–11.

Nowacki, D. J., Ogston, A.S., Nittrouer, C. A., Fricke, A. T., & Van, P. D. T. (2015). Sediment dynamics in the lower Mekong river: Transition from tidal river to estuary. *Journal of Geophysical Research: Oceans*, *120*, 6363–6383.

Otsuka, J., Saruwatari, A., & Watanabe, Y. (2017). Vortex-induced suspension of sediment in the surf zone. *Advances in Water Resources*, *110*, 59–76.

Pal, D., & Ghoshal, K. (2016). Effect of particle concentration on sediment and turbulent diffusion coefficients in open-channel turbulent flow. *Environmental Earth Sciences*, *75*, 1–11.

Park, E., & Latrubesse, E. M. (2015). Surface water types and sediment distribution patterns at the confluence of mega rivers: The Solimões-Amazon and Negro Rivers junction. *Water Resources Research*, *51*, 6197–6213.

Reyes-Marambio, J., Moser, F., Gana, F., Severino, B., Calderón-Muñoz, W. R., Palma-Behnke, R., Estevez, P. A., Orchard, M., & Cortés, M. (2016). A fractal time thermal model for predicting the surface temperature of air-cooled cylindrical Li-ion cells based on experimental measurements. *Journal of Power Sources*, *306*, 636–645.

Rouse, H. (1937). Modern conceptions of the mechanics of fluid turbulence. *Transactions of the American Society of Civil Engineers*, *102*, 463–505.

Sreenivasan, K., & Meneveau, C. (1986). The fractal facets of turbulence. *Journal of Fluid Mechanics*, *173*, 357–386.

Sun, H., & Chen, W. (2009). Fractal derivative multi-scale model of fluid particle transverse accelerations in fully developed turbulence. *Science China Technological Sciences*, *52*, 680–683.

Sun, H., Li, Z., Zhang, Y., & Chen, W. (2017). Fractional and fractal derivative models for transient anomalous diffusion: Model comparison. *Chaos, Solitons & Fractals*, *102*, 346–353.

Sun, H., Meerschaert, M. M., Zhang, Y., Zhu, J., & Chen, W. (2013). A fractal Richards' equation to capture the non-Boltzmann scaling of water transport in unsaturated media. *Advances in Water Resources*, *52*, 292–295.

Umeyaina, M. (1992). Vertical distribution of suspended sediment in uniform open-channel flow. *Journal of Hydraulic Engineering*, *118*, 936–941.

Vanoni, V. A., & Brooks, N. H. (1957). Laboratory studies of the roughness and suspended load of alluvial streams. California Institute of Technology Sedimentation Laboratory, Sediment Series No. 11, Omaha, NE. U.S. Army Crops of Engineers, Missouri River Division.

van Rijn, L. C. (1984). Sediment transport, part II: Suspended load transport. *Journal of Hydraulic Engineering*, *110*, 1613–1641.

Wang, G., & Fu, X. (2004). Mechanisms of particle vertical diffusion in sediment-laden flows. *Chinese Science Bulletin*, *49*, 1086–1090.

Wang, G., & Ni, J. (1991). The kinetic theory for dilute solid/liquid two-phase flow. *International Journal of Multiphase Flow*, *17*, 273–281.

Wang, X., & Qian, N. (1989). Turbulence characteristics of sediment-laden flow. *Journal of Hydraulic Engineering*, *115*, 781–800.

Wang, X., & Qian, N. (1992). Velocity profiles of sediment laden flow. *International Journal of Sediment Research*, *7*, 27–58.

Yu, X., Zhang, Y., Sun, H., & Zheng, C. (2018). Time fractional derivative model with Mittag-Leffler function kernel for describing anomalous diffusion: Analytical solution in bounded-domain and model comparison. *Chaos, Solitons & Fractals*, *115*, 306–312.

Zhang, R. (1998). *River sediment dynamics*. Beijing: China Water and Power Press.

Zhang, Y. (2010). Moments for tempered fractional advection-diffusion equations. *Journal of Statistical Physics*, 139, 915–939.

Zhang, Y., & Meerschaert, M. M. (2011). Gaussian setting time for solute transport in fluvial systems. *Water Resources Research*, *47*, 1–6.

Zheng, J., Li, R., & Feng, Q. (2012). Vertical distribution of nearshore sediment concentration. *Applied Mechanics and Materials*, *170*, 2272–2275.

Zhou, W., Sornette, D., & Yuan, W. (2006). Inverse statistics and multifractality of exit distances in 3D fully developed turbulence. *Physica D: Nonlinear Phenomena*, *214*, 55–62.

Figure

Click here to access/download;Figure;Fig. 1.jpg

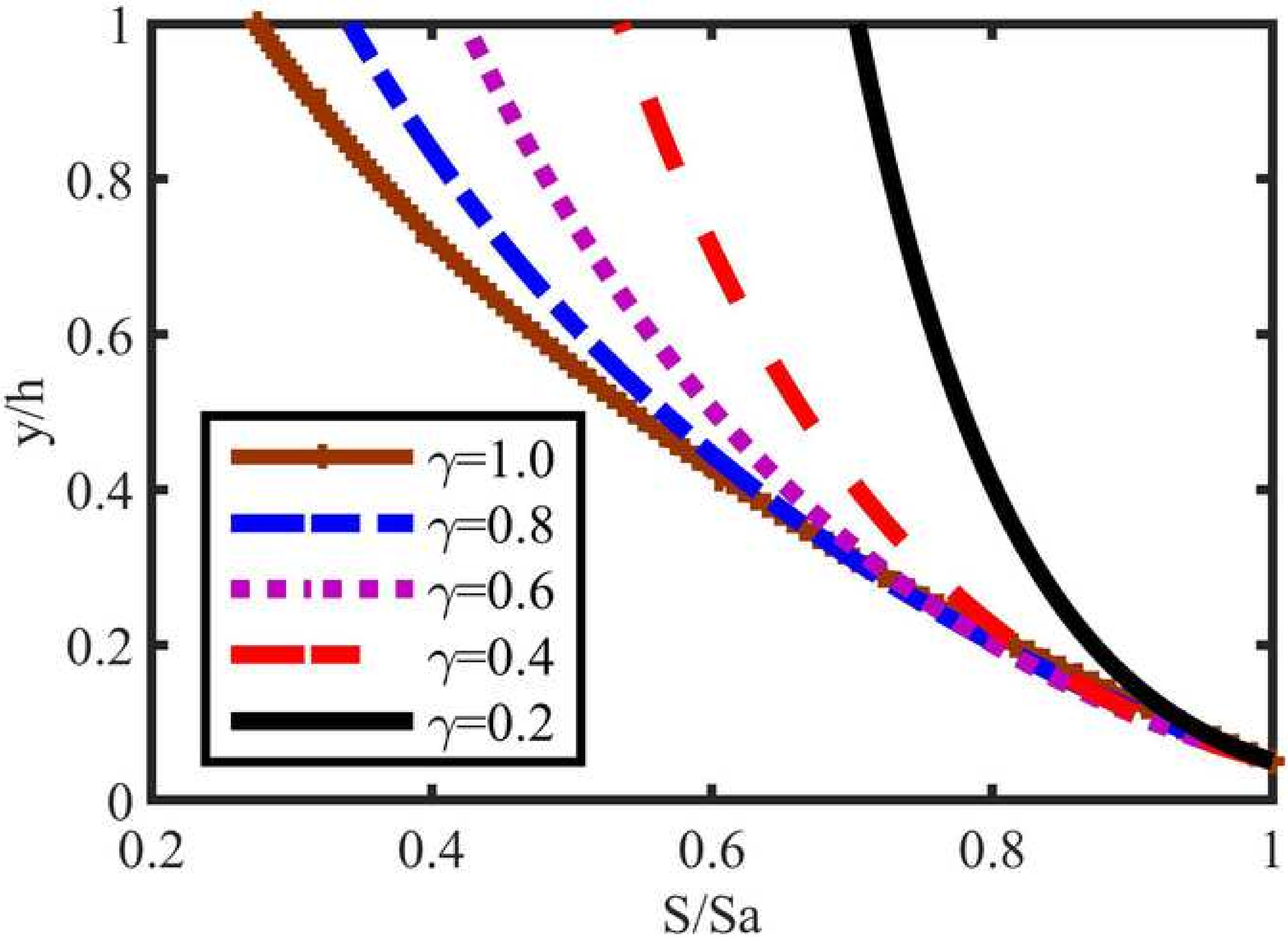

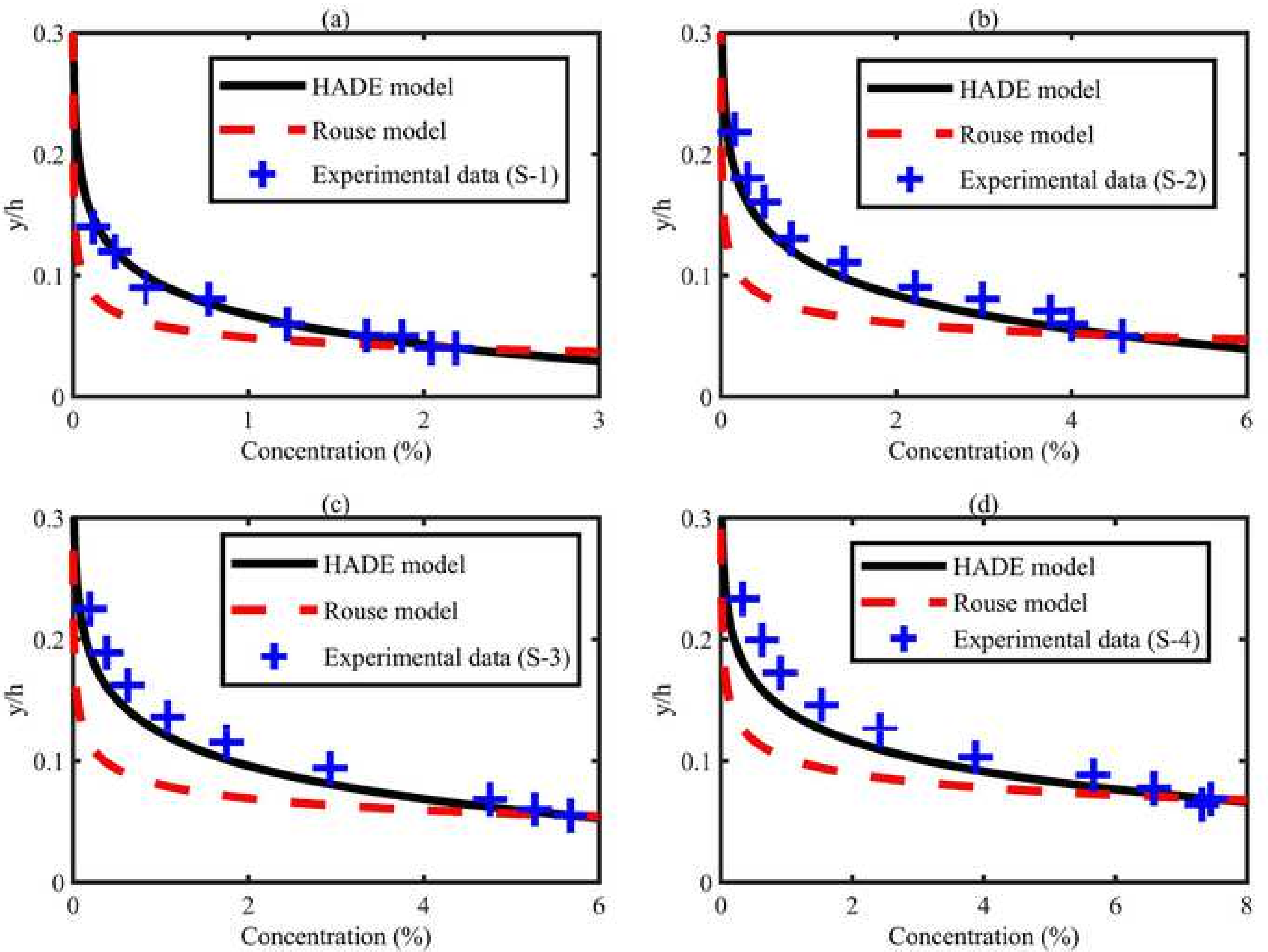
(a)
(b)
(c)
(d)
HADE model
Rouse model
Experimental data (S-1)
Experimental data (S-2)
Experimental data (S-3)
Experimental data (S-4)
y/h
Concentration (%)
0.3
0.2
0.1
0
1
2
3
4
6
8

Figure

Click here to access/download;Figure;Fig. 3.jpg

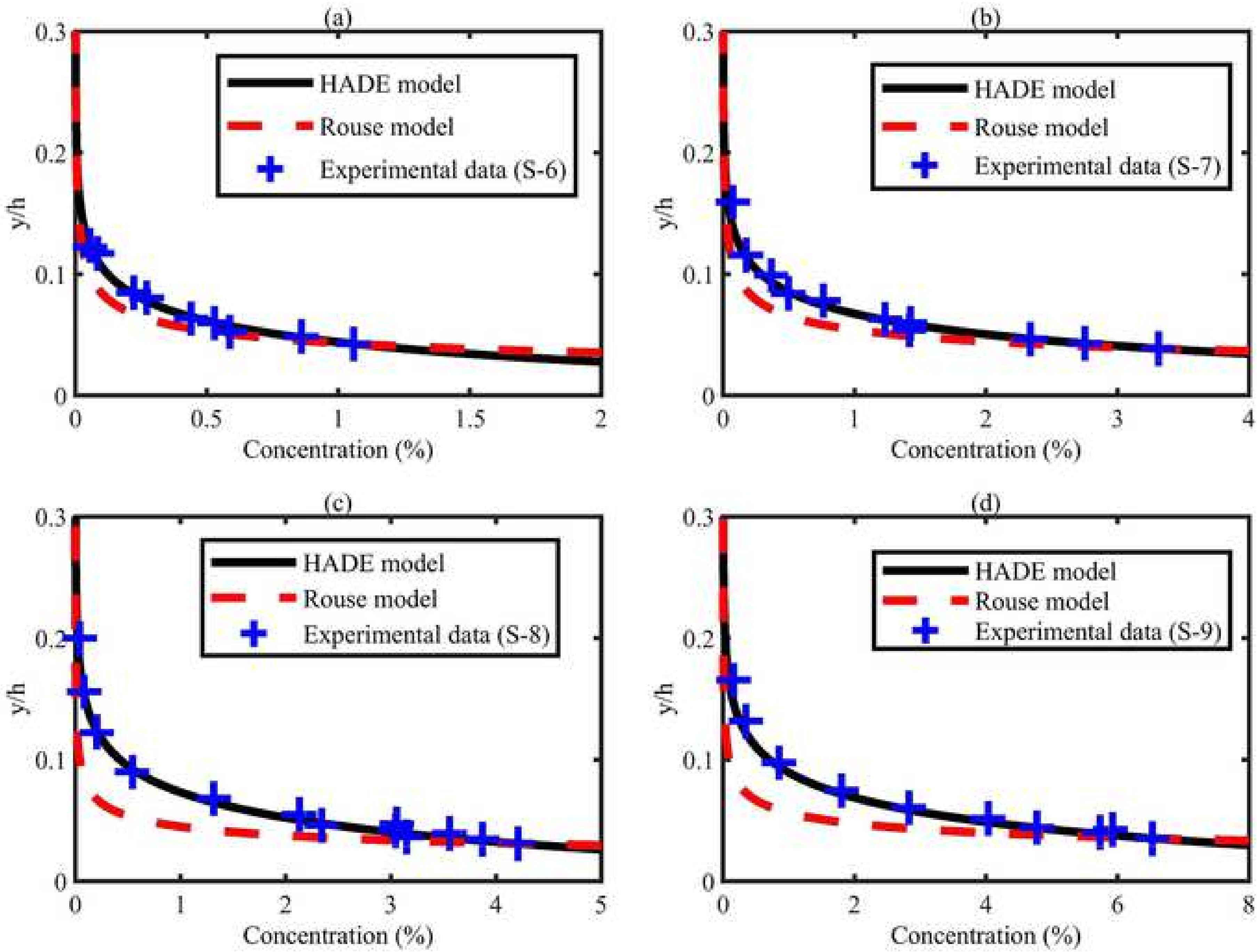

Figure

Click here to access/download;Figure;Fig. 4.jpg

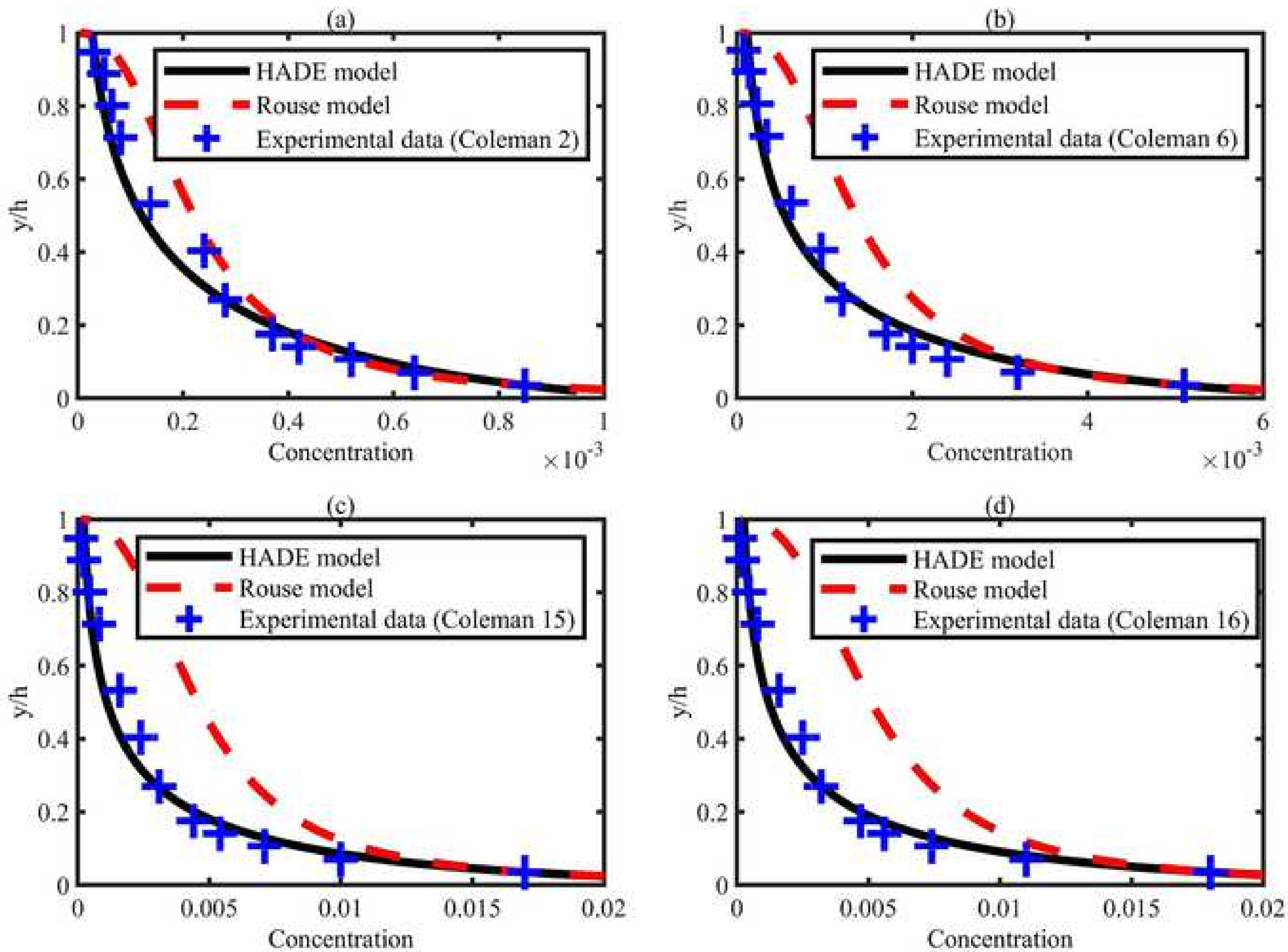

Figure

Click here to access/download;Figure;Fig. 5.jpg

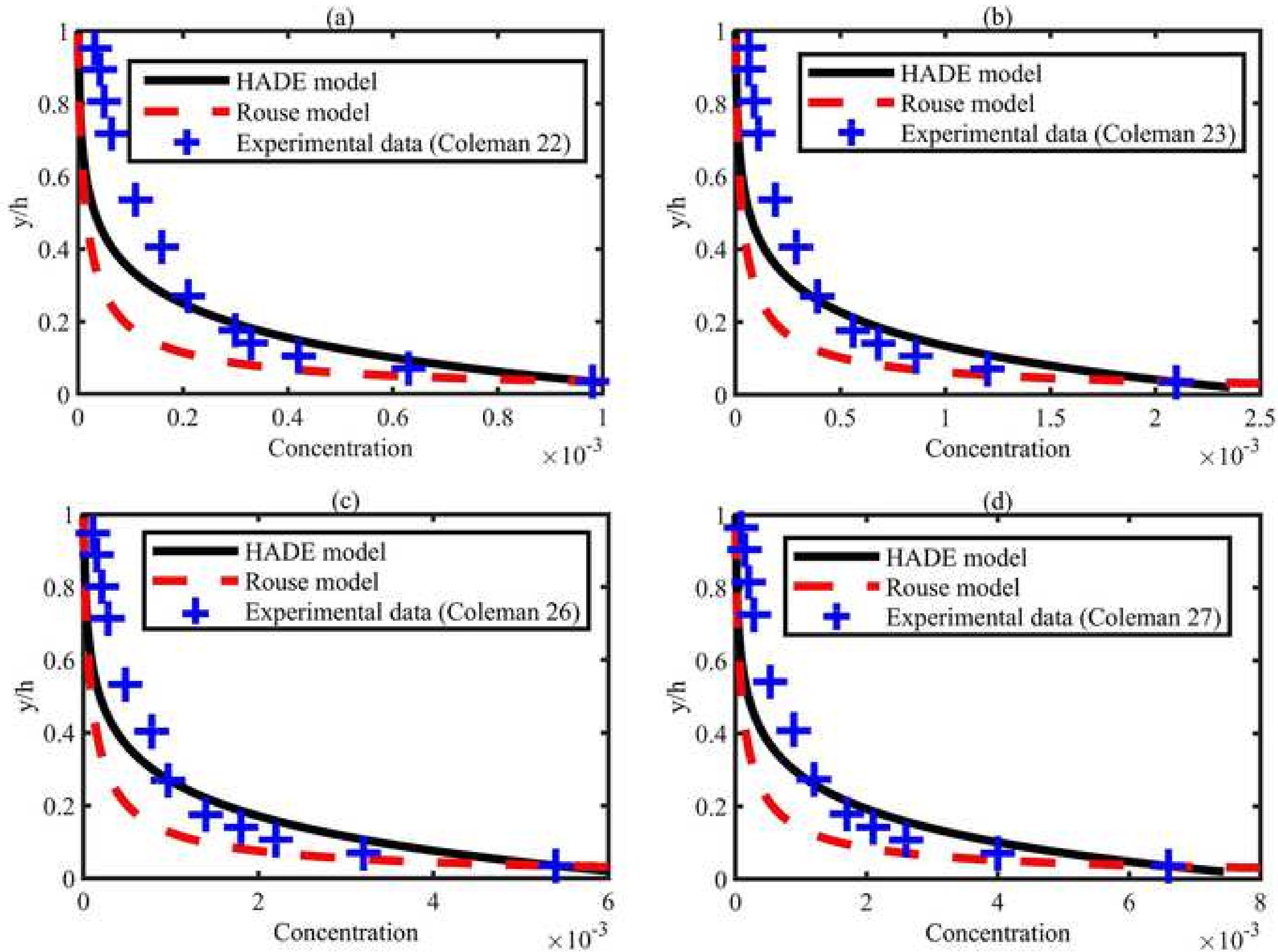

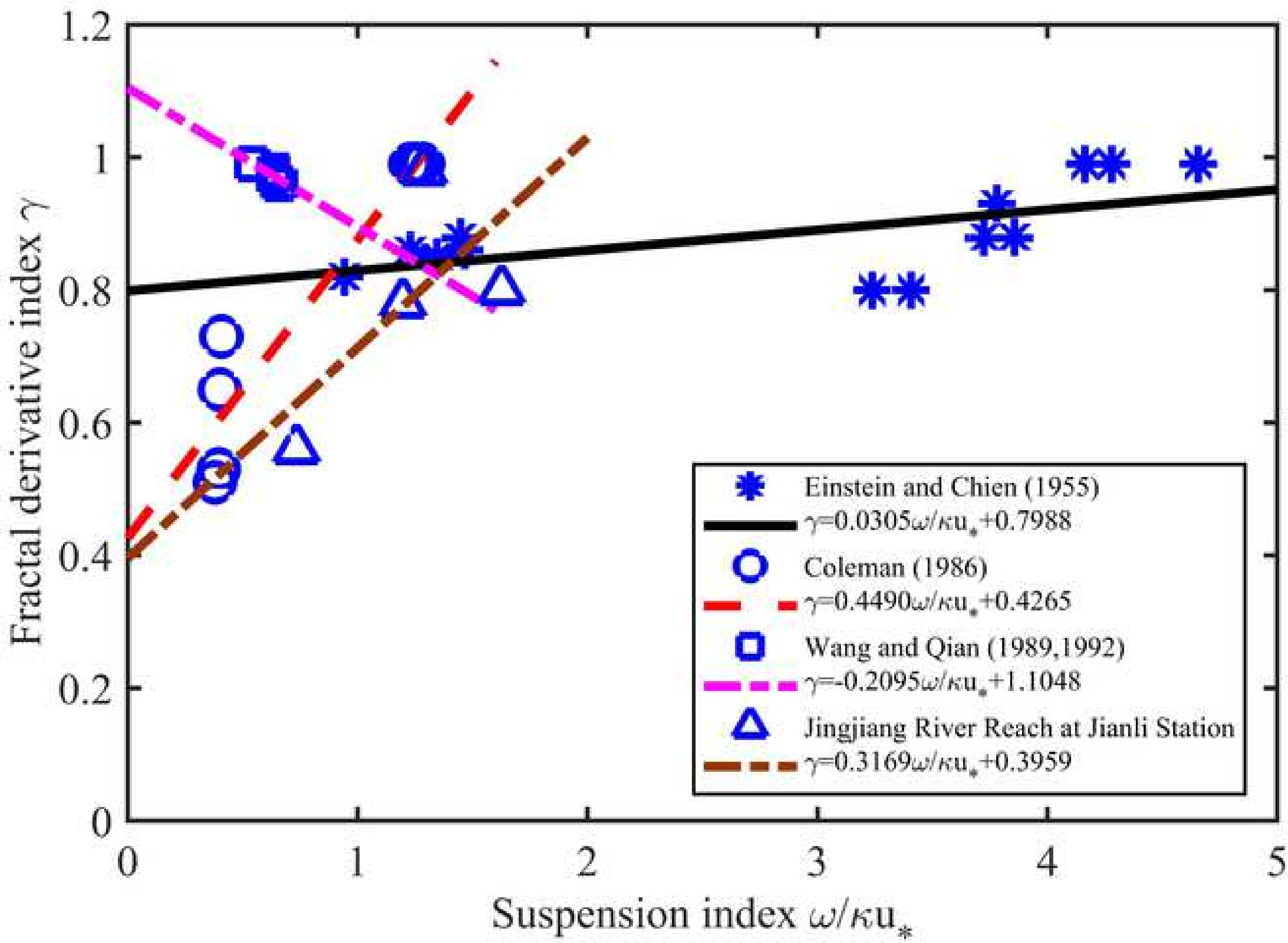
1.2
1
0.8
0.6
0.4
0.2
0
0
1
2
3
4
5
Fractal derivative index γ
Suspension index ω/κu*
Einstein and Chien (1955)
γ=0.0305ω/κu*+0.7988
Coleman (1986)
γ=0.4490ω/κu*+0.4265
Wang and Qian (1989,1992)
γ=-0.2095ω/κu*+1.1048
Jingjiang River Reach at Jianli Station
γ=0.3169ω/κu*+0.3959

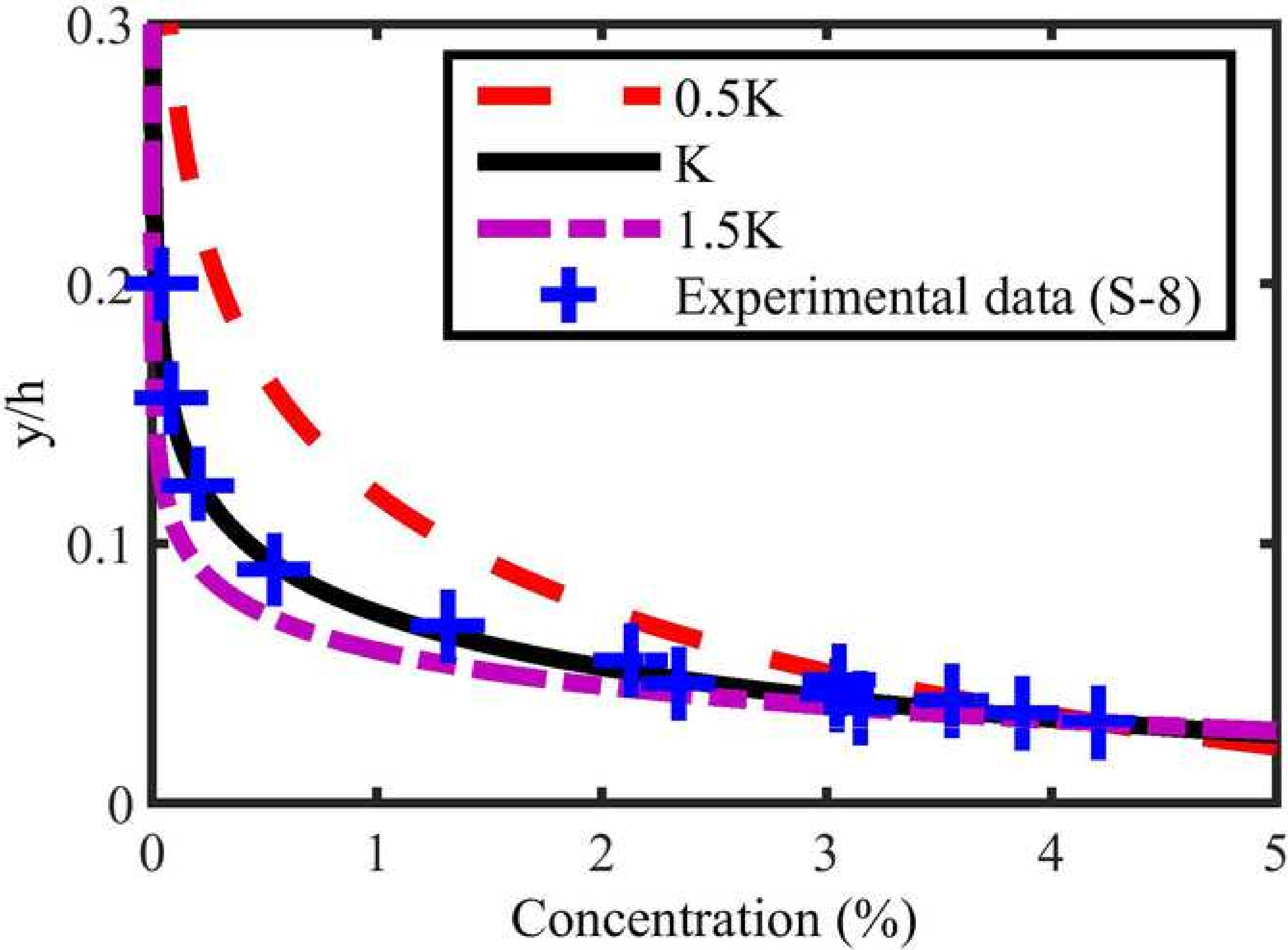
0.5K
K
1.5K
Experimental data (S-8)
y/h
Concentration (%)
0.3
0.2
0.1
0
0
1
2
3
4
5

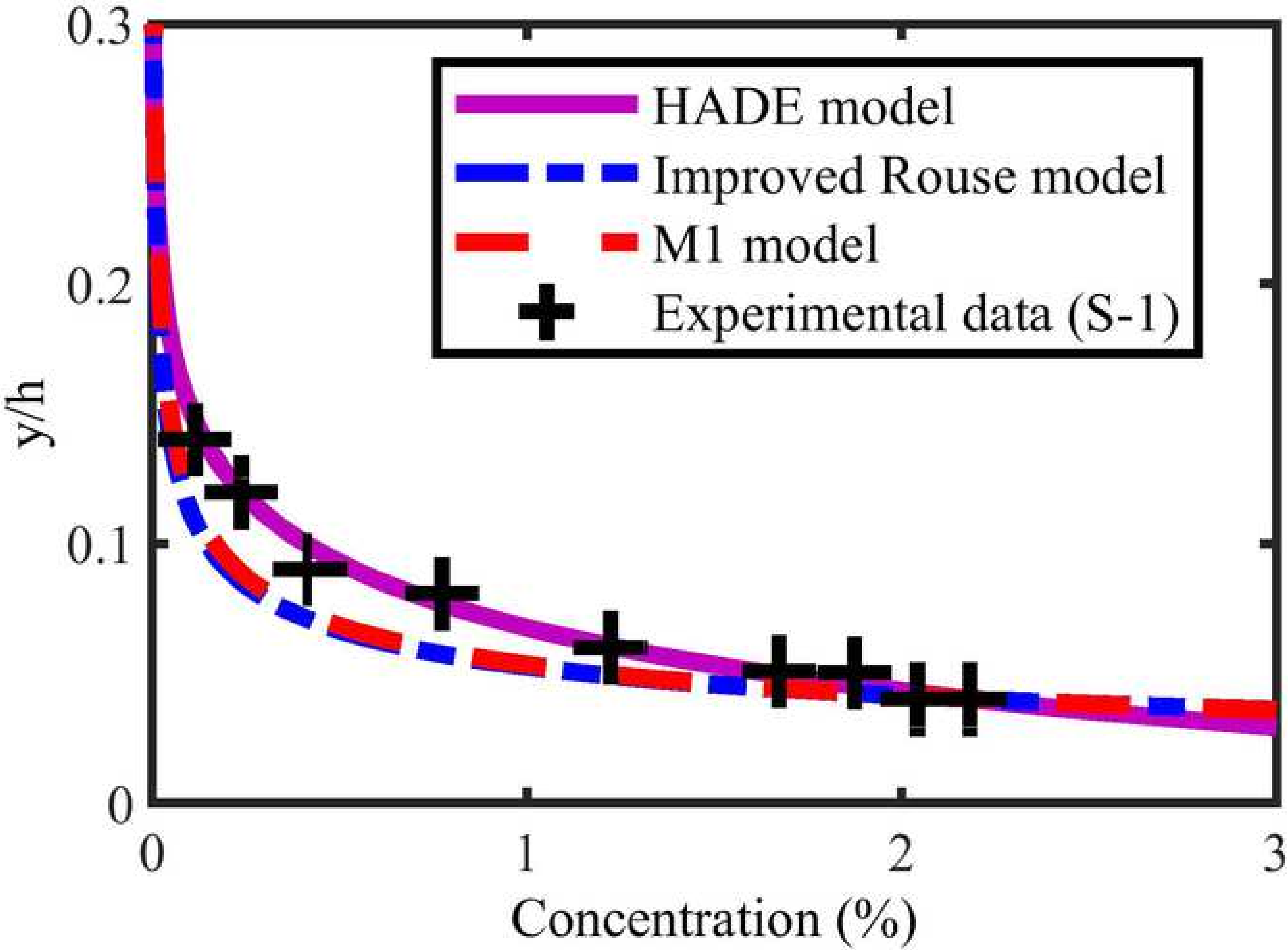
0.3
0.2
0.1
0
y/h
0
1
2
3
Concentration (%)
HADE model
Improved Rouse model
M1 model
Experimental data (S-1)

Figure

Click here to access/download;Figure;Fig. 9.jpg

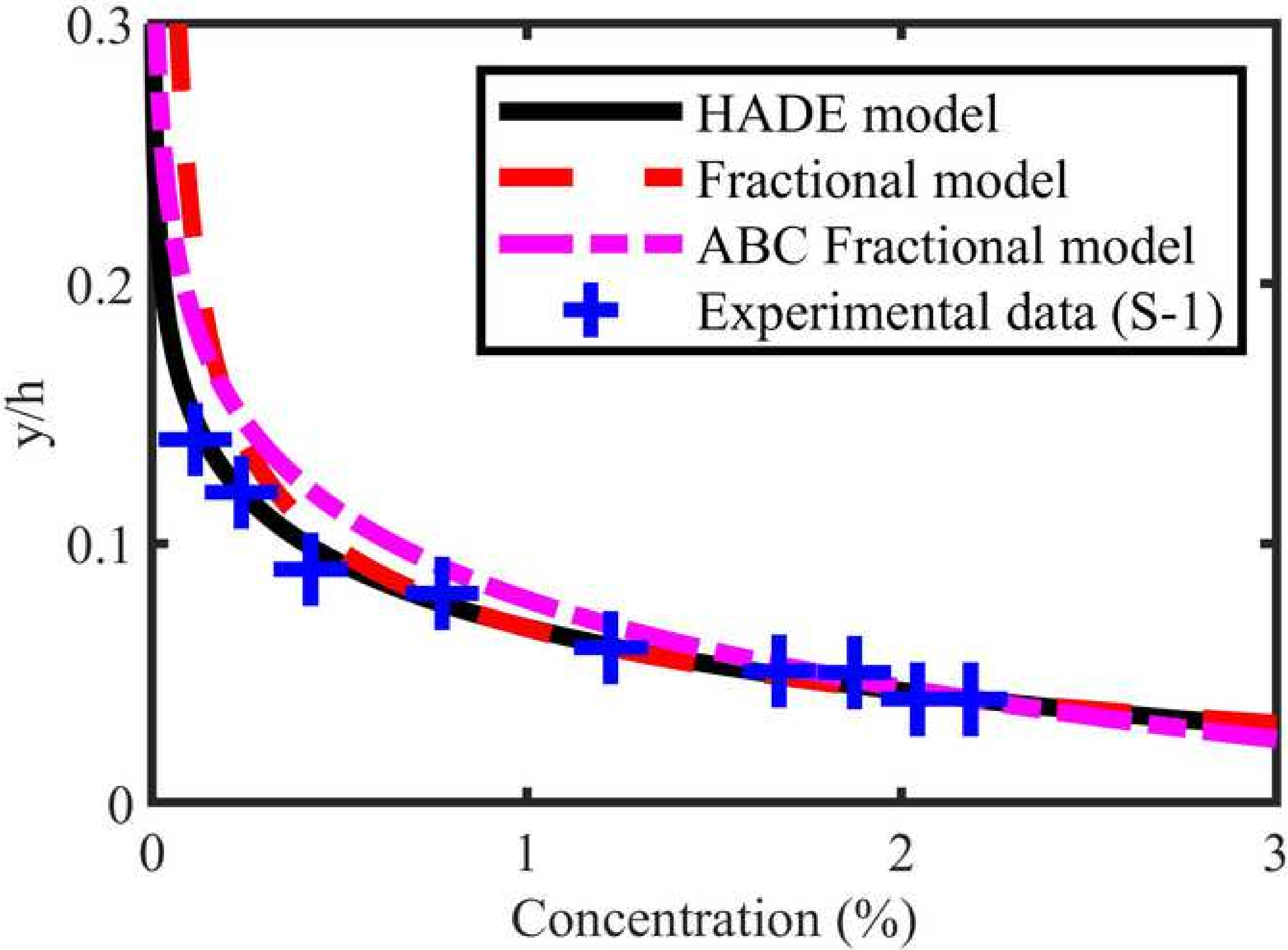

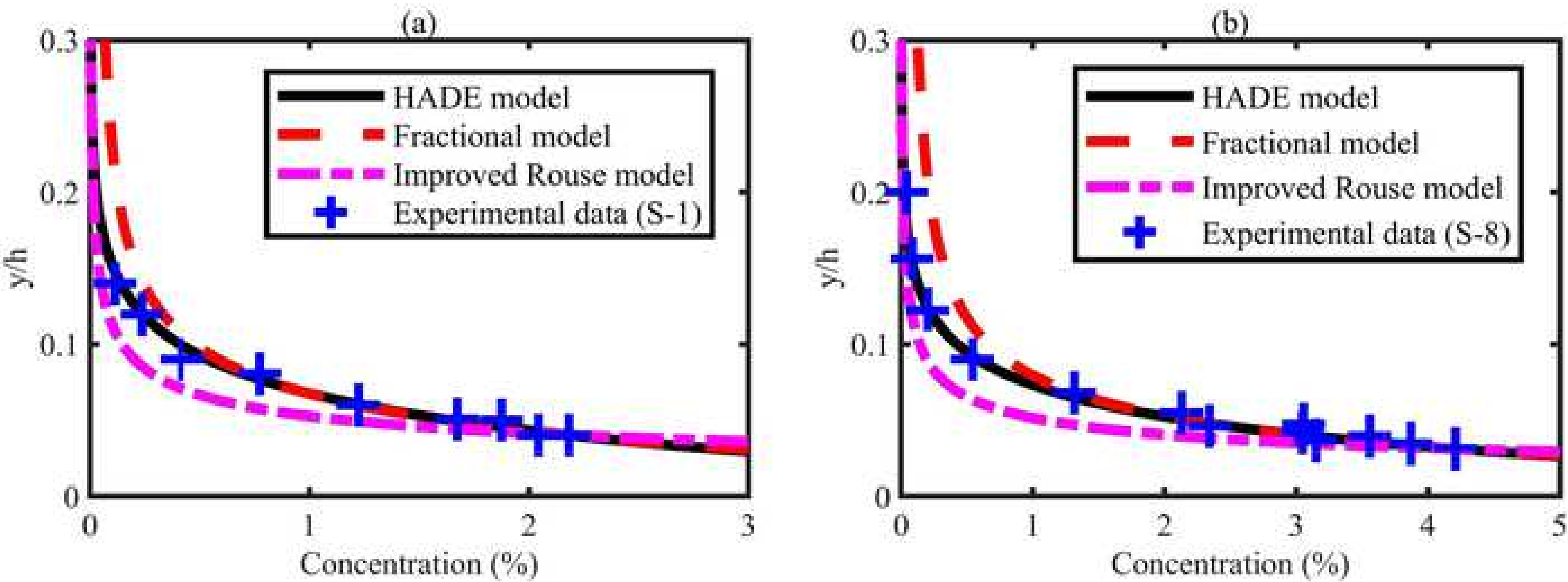
(a)
0.3
0.2
0.1
0
y/h
0
1
2
3
Concentration (%)
HADE model
Fractional model
Improved Rouse model
Experimental data (S-1)
(b)
0.3
0.2
0.1
0
y/h
0
1
2
3
4
5
Concentration (%)
HADE model
Fractional model
Improved Rouse model
Experimental data (S-8)

Figure

Click here to access/download;Figure;Fig. A1.jpg

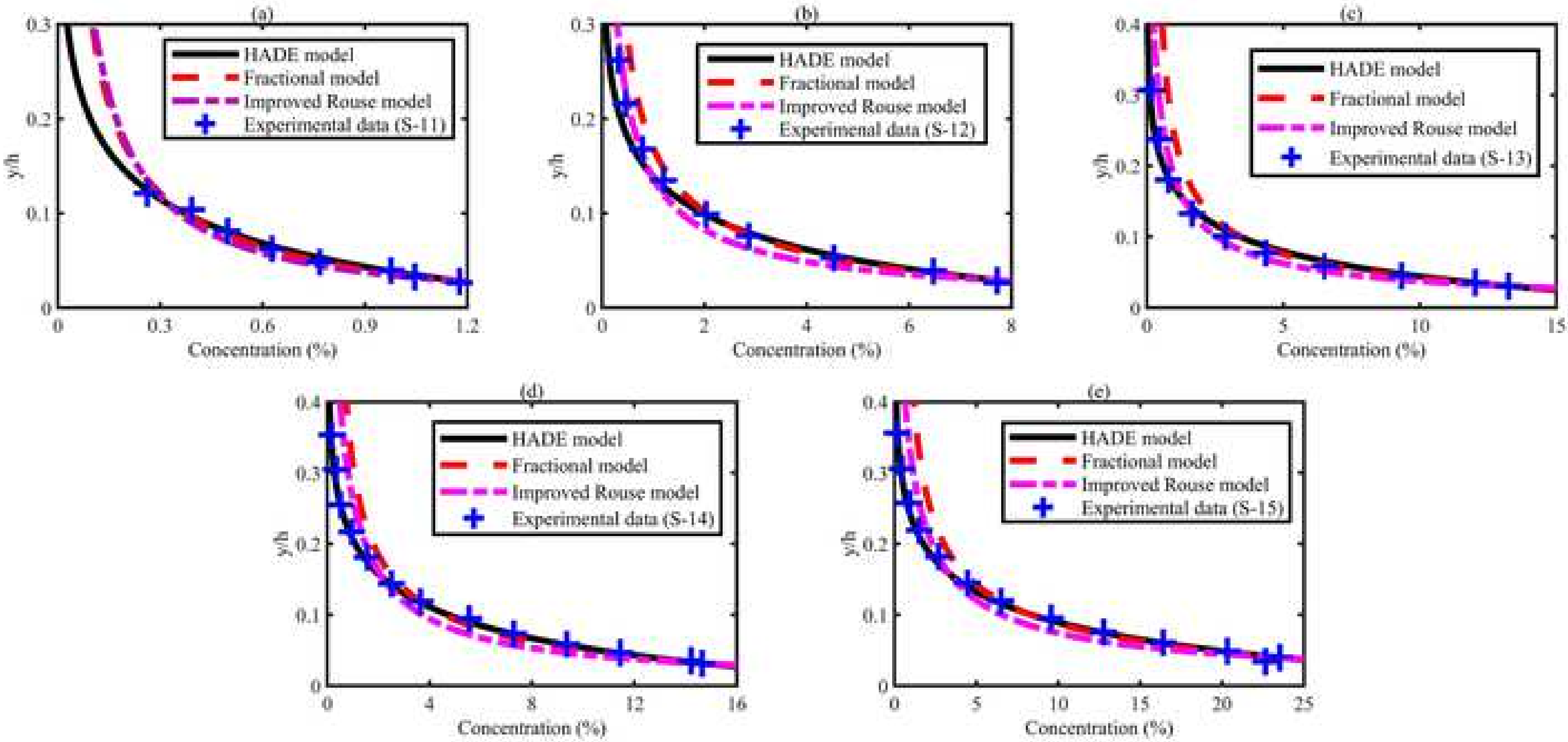

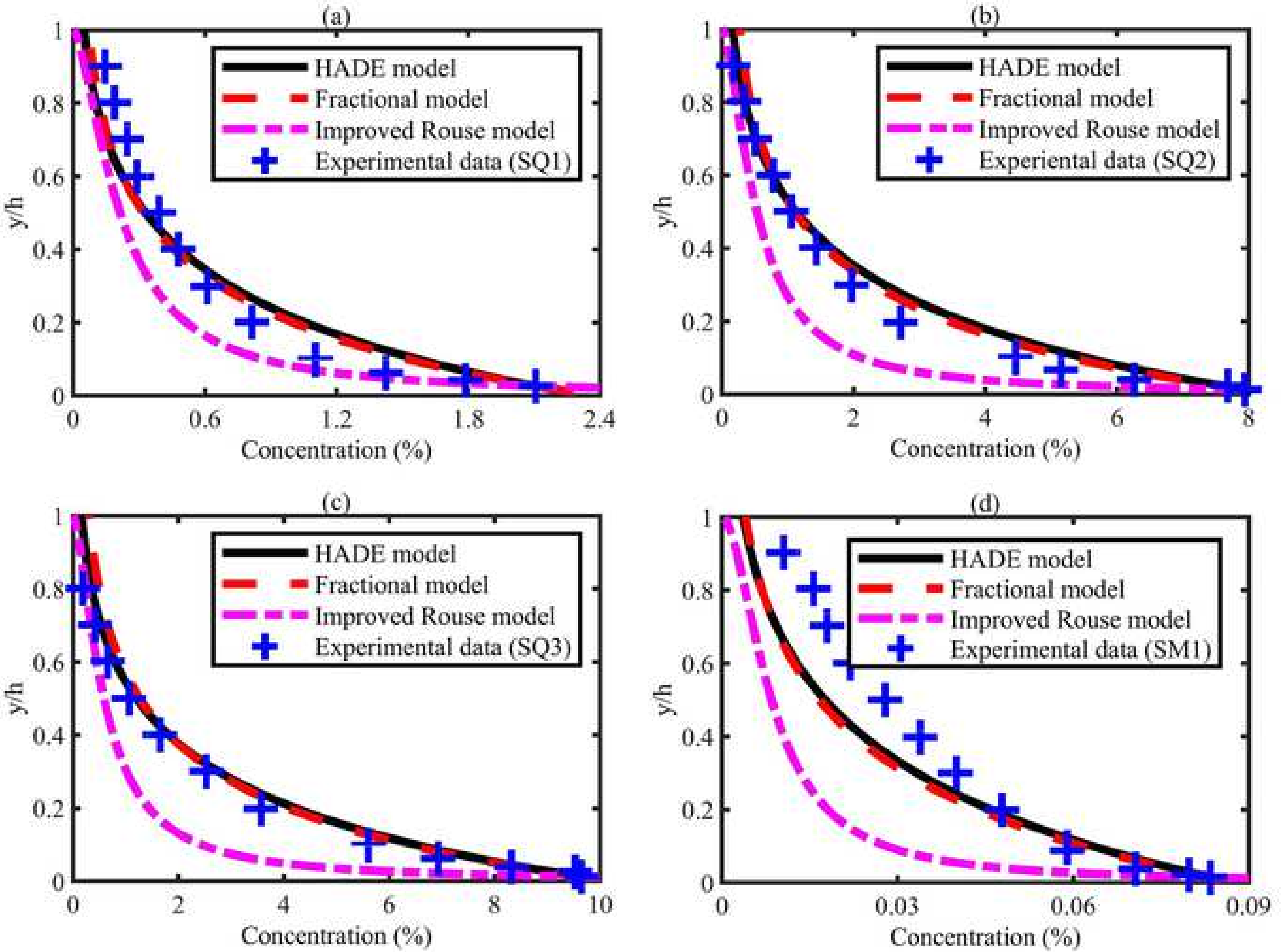
(a)
HADE model
Fractional model
Improved Rouse model
Experimental data (SQ1)
y/h
Concentration (%)
0
0.2
0.4
0.6
0.8
1
0.6
1.2
1.8
2.4
(b)
HADE model
Fractional model
Improved Rouse model
Experiental data (SQ2)
y/h
Concentration (%)
2
4
6
8
(c)
HADE model
Fractional model
Improved Rouse model
Experimental data (SQ3)
y/h
Concentration (%)
10
(d)
HADE model
Fractional model
Improved Rouse model
Experimental data (SM1)
y/h
Concentration (%)
0.03
0.06
0.09

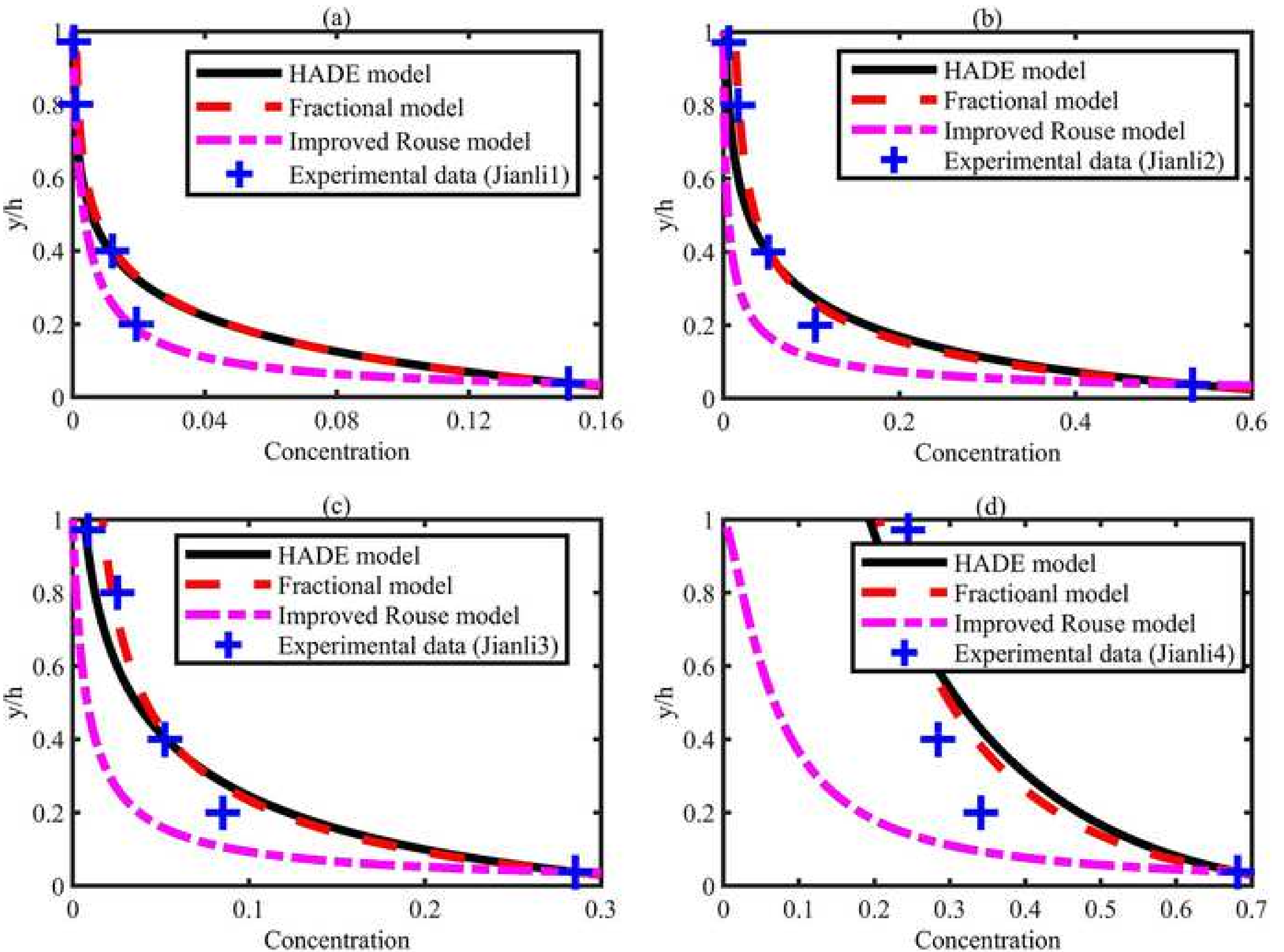
(a)
HADE model
Fractional model
Improved Rouse model
Experimental data (Jianli1)
y/h
Concentration
0
0.04
0.08
0.12
0.16
0.2
0.4
0.6
0.8
1
(b)
HADE model
Fractional model
Improved Rouse model
Experimental data (Jianli2)
y/h
Concentration
0.2
0.4
0.6
(c)
HADE model
Fractional model
Improved Rouse model
Experimental data (Jianli3)
y/h
Concentration
0.1
0.2
0.3
(d)
HADE model
Fractioanl model
Improved Rouse model
Experimental data (Jianli4)
y/h
Concentration
0.1
0.2
0.3
0.4
0.5
0.6
0.7